The Small Muscle-specific Protein Csl Modifies Cell Shape and Promotes Myocyte Fusion in an Insulin-like Growth Factor 1–dependent Manner

Steve Palmer,* Nicola Groves,* Aaron Schindeler,* Thomas Yeoh,* Christine Biben,* Cheng-Chun Wang,* Duncan B. Sparrow,* Louise Barnett,‡ Nancy A. Jenkins,§ Neal G. Copeland,§ Frank Koentgen,‡ Tim Mohun,‖ and Richard P. Harvey*¶

*Victor Chang Cardiac Research Institute, Darlinghurst, NSW 2010, Australia; ‡Walter and Eliza Hall Institute of Medical Research, Melbourne, Victoria 3050, Australia; §Mouse Cancer Genetics Program, National Cancer Institute-Frederick, Frederick, Maryland 21702; ‖Medical Research Council Institute for Medical Research, London NW7 1AA, United Kingdom; and ¶Faculties of Medicine and Life Sciences, University of New South Wales, Kensington, NSW 2051, Australia

Abstract. We have isolated a murine cDNA encoding a 9-kD protein, Chisel (Csl), in a screen for transcriptional targets of the cardiac homeodomain factor Nkx2-5. *Csl* transcripts were detected in atria and ventricles of the heart and in all skeletal muscles and smooth muscles of the stomach and pulmonary veins. Csl protein was distributed throughout the cytoplasm in fetal muscles, although costameric and M-line localization to the muscle cytoskeleton became obvious after further maturation. Targeted disruption of *Csl* showed no overt muscle phenotype. However, ectopic expression in C2C12 myoblasts induced formation of lamellipodia in which Csl protein became tethered to membrane ruffles. Migration of these cells was retarded in a monolayer wound repair assay. Csl-expressing myoblasts differentiated and fused normally, although in the presence of insulin-like growth factor (IGF)-1 they showed dramatically enhanced fusion, leading to formation of large dysmorphogenic "myosacs." The activities of transcription factors nuclear factor of activated T cells (NFAT) and myocyte enhancer–binding factor (MEF)2, were also enhanced in an IGF-1 signaling–dependent manner. The dynamic cytoskeletal localization of Csl and its dominant effects on cell shape and behavior and transcription factor activity suggest that Csl plays a role in the regulatory network through which muscle cells coordinate their structural and functional states during growth, adaptation, and repair.

Key words: costameres • heart • lamellipodia • Nkx2-5 • skeletal muscle

Introduction

The mammalian heart is an organ of considerable structural and regulatory complexity. Emphasis is now being placed on unraveling the genetic circuitry underlying cardiac patterning and morphogenesis and how this relates to congenital disease (Fishman and Chien, 1997). A key gene in the myocardial developmental regulatory hierarchy in vertebrates is *Nkx2-5*, a homologue of the *Drosophila* homeobox gene, *tinman,* essential for specification of the heart and visceral muscle lineages in the fly (Harvey, 1996). *Nkx2-5* can promote cardiogenesis in vitro (Skerjanc et al., 1998) and to a limited extent in vivo (Cleaver et al., 1996) and can rescue some of the functions of *tinman* when expressed as a transgene in *tinman*-mutant *Drosophila* embryos (Park et al., 1998; Ranganayakulu et al., 1998). In frogs, dominant negative inhibition of Nkx2-5 leads to complete obliteration of heart formation, suggesting an essential role in specification of the cardiac lineages in this vertebrate (Fu et al., 1998; Grow and Krieg, 1998). Homozygous mutations in murine *Nkx2-5* lead to arrest of cardiac morphogenesis at the linear heart tube stage (Lyons et al., 1995; Tanaka et al., 1999; Biben et al., 2000), whereas heterozygous mutations in both the human and mouse genes confer atrial septal defects and conduction abnormalities (Schott et al., 1998; Biben et al., 2000). Nkx2-5 is thought to act, in part, via its association with the transcription factors GATA4 (Durocher et al., 1997) and serum response factor (Chen and Schwartz, 1996), and in vivo and/or in vitro studies have identified *atrial natriuretic factor*, *A1 adenosine receptor*, *calreticulin*, and *α-cardiac actin* as direct target genes (Chen and Schwartz, 1996; Durocher et al., 1996; Biben et al., 1997; Rivkees et al., 1999;

Address correspondence to Richard P. Harvey, Victor Chang Cardiac Research Institute, 384 Victoria St., Darlinghurst 2010, NSW, Australia. Tel.: 61-2-9295-8520. Fax: 61-2-9295-8528. E-mail: r.harvey@victorchang.unsw.edu.au

F. Koentgen's present address is Ozgene, Australian Gene Targeting Center, Nedlands 6009, Australia.

S. Palmer's present address is The Institute of Cancer Research, London SW 36JB, UK.

C.-C. Wang's present address is Institute of Molecular and Cell Biology, Singapore 117609.

Guo et al., 2000). However, in knockout mice genes encoding the regionally expressed transcription factors Hand1/eHand, Irx4, Msx-2, and N-myc and the actin cross-linking protein SM-22α are also dysregulated (Biben and Harvey, 1997; Biben et al., 1997; Tanaka et al., 1999; Bruneau et al., 2000), suggesting a role for Nkx2-5 in the development of patterning information and heart tube morphogenesis.

In this paper, we describe the gene *Chisel* (*Csl*),[1] which was cloned during a differential screen for genes downregulated in homozygous *Nkx2-5* mutant hearts. *Csl* encodes a protein of 9 kD expressed in the heart, all skeletal muscles, and smooth muscles of the stomach and pulmonary veins. In the heart, *Csl* transcripts were expressed only in the specialized working myocardium of the atrial and ventricular chambers. Although *Csl* knockout mice showed no obvious phenotype, over-expression in the C2C12 myogenic cell line led to effects on cytoskeletal dynamics in myoblasts and cell signaling–dependent enhancement of cell fusion in myocytes. The activities of nuclear factor of activated T cells (NFAT) and myocyte enhancer–binding factor (MEF)2 transcription factors were also enhanced in a cell signaling–dependent manner. These data suggest that Csl acts in the signaling network through which the structural, functional, and regulatory states of muscle cells are coordinated.

Materials and Methods

DNA and RNA Analysis

RNase protections were performed according to Ambion methods. *Csl* probe corresponded to residues 257–392 of the cDNA (see Fig. 1). *Cyclophilin* probe was synthesized from a template obtained from Ambion. In situ hybridization was performed as described (Biben and Harvey, 1997). *Csl* probe corresponded to bases 9–787 of the cDNA (see Fig. 1). Oligonucleotides used for genotyping knockout mice were: common forward primer, 5′-ccttgaatctgaaggctgcc-3′; wild-type reverse, 5′-cgttcaggacccacatgaag-3′; *fAP* allele reverse, 5′-ccatcagaagctgactctag-3′; and *AP*Δ allele reverse, 5′-tctgtgcaggctgcagcttc-3′.

Production of an Anti-Csl Antibody

Glutathione *S*-transferase (GST)–Csl fusion protein was produced from pGEX-2T (Amersham Pharmacia Biotech). Fusion protein was cleaved from a glutathione–Sepharose 4B column (Amersham Pharmacia Biotech) using 5 U/ml thrombin (Amersham Pharmacia Biotech) at 4°C overnight. Two rabbits were immunized with 600 μg of recombinant Csl in Freund's Adjuvant (1:1) and boosted with 600 μg monthly (Institute of Medical and Veterinary Science, Adelaide, Australia). IgG fraction was purified on protein G–Sepharose (Pharmacia Amersham Biotech). Since IgG from both rabbits contained antibodies that cross-reacted with desmin, Csl antibody was routinely immunoabsorbed against desmin fusion protein (amino acids 412–470).

Western Blot Analysis

PVDF membranes (Millipore) were blocked with 0.05% Tween 20, 2% bovine serum albumin, PBS. Csl antibody (1:1,500) was followed by anti–rabbit IgG conjugated to HRP (1:1,000; Silenus). mAbs anti-Hsp 70 (1:1,000; Sigma-Aldrich) and anti-Akt (1:2,000; New England Biolabs, Inc.) were used with anti–mouse IgG–HRP (Silenus). Bands were detected by chemiluminescence (Amersham Pharmacia Biotech).

[1]*Abbreviations used in this paper:* CsA, cyclosporine A; Csl, Chisel; GFP, green fluorescent protein; GST, glutathione *S*-transferase; hPAP, human placental alkaline phosphatase; IGF, insulin-like growth factor; MEF, myocyte enhancer–binding factor; MLC, myosin light chain; NFAT, nuclear factor of activated T cells; PFA, paraformaldehyde.

Cell Culture

Csl cDNA was cloned into pEF FLAG A (a gift from David Huang, Walter and Eliza Hall Institute of Medical Research, Parkville, Victoria, Australia), pEFBosMyc (a gift from N. Nicola, Walter and Eliza Hall Institute of Medical Research), pEGFP-C1 (CLONTECH Laboratories, Inc.), and a vector carrying a myosin light chain (MLC)1 promoter/enhancer (Musaro and Rosenthal, 1999). Activated calcineurin A was cloned into pPGKpuropAv18 (a gift from David Huang). Transfections were performed with lipofectamine (GIBCO BRL) according to instructions. pEF FLAG A was used at 10:1 for puromycin selection where necessary. Two sublines of C2C12 cells were used. FLAG-Csl lines were made from stocks held at the Walter and Eliza Hall Institute of Medical Research and grown as described (Semsarian et al., 1999). Myc-Csl lines were made in cells from the laboratory of H. Blau (Stanford University, Palo Alto, CA) and grown in low glucose DME, 20% FBS, and 0.5% chick embryo extract. In transfections, reporter plasmids were cotransfected with an SV40-LacZ expression plasmid (9:1) for normalization. Luciferase activity was determined using Promega reagents. Flow cytometry was performed on a Becton Dickinson FACSCalibur™.

Immunofluorescence

C2C12 cells on coverslips were fixed in ice-cold acetone for 15 min or in 4% paraformaldehyde (PFA)/PBS for a minimum of 15 min, followed by 0.5% Triton X-100/PBS for 15 min as appropriate for each antigen. For cryosections, tissue was embedded in OCT compound (Tissue-Tek) and immersed in isopentane cooled almost to the point of solidity using liquid nitrogen. Sections were fixed in ice-cold acetone or 4% PFA/PBS for 15 min. Antibodies were as follows: anti–α-actinin mouse mAb (Sigma-Aldrich) (EA-53, 1:100; acetone/PFA fixation); antimyosin heavy chain IIb mouse IgM mAb (supplied by Edna Hardeman, Children's Medical Research Institute, Wentworthville, New South Wales, Australia) (neat; acetone fixation); anti-Csl rabbit polyclonal (1:200; PFA); antimyosin heavy chain mAb (MF20; Developmental Studies Hybridoma Bank) (1:20; acetone); antitalin mAb (Sigma-Aldrich) (1:20; PFA); antimyosin heavy chain I/slow mAb (supplied by Edna Hardeman) (neat; PFA); anti-myc epitope mAb (9E10; Developmental Studies Hybridoma Bank) (1:10; PFA). Confocal images were obtained using a Leica TCS NT system. Photomicrographs were prepared using a Spot-II digital system (Diagnostics Instruments).

Calcineurin Assays

Calcineurin activity was assayed as described (Semsarian et al., 1999) using okadaic acid at 1 μM and calmodulin at 250 nM. Calcineurin activity was calculated as the difference between total phosphatase activity on target peptide (Auspep) with and without 1 μM cyclosporine A (CsA) added to cells 20 min before preparation of extracts or with and without addition of calcineurin autoinhibitory peptide (500 μM) (Calbiochem) to extracts.

Wounding Assays

Parallel 150-μm wounds were made in confluent monolayers using a flame-polished glass needle on a micromanipulator. After 6 h in culture, cells were fixed (4% PFA/PBS) and stained (1% eosin). Wound areas were measured before and after culture using Leica Q500MC software.

Results

Cloning of Mouse Csl

A cDNA fragment encoding a novel protein termed Csl (cardiac and skeletal muscle protein) was cloned during a differential screen for transcriptional targets of the cardiac-expressed homeodomain factor Nkx2-5 (Harvey, 1996). The basis of the screen was a targeted mouse line carrying a null allele of *Nkx2-5* (*Nkx2-5^{HDneo}*) (Lyons et al., 1995; Biben et al., 2000). Hearts from wild-type and homozygous mutant embryos were dissected at embryonic day (E)8.5, and total RNA was extracted and converted to cDNA using the CapFinder PCR cDNA synthesis kit (CLONTECH Laboratories, Inc.). cDNAs were then am-

plified using PCR and used in a suppression subtractive hybridization procedure (PCR-Select; CLONTECH Laboratories, Inc.). Selective PCR amplification of differentially expressed products yielded several fragments, one of which encoded Csl. Hybridization of a *Csl* probe to Southern filters carrying an equal mass of mutant and wild-type cDNAs demonstrated that *Csl* was downregulated more than 20 times in the mutant context (data not shown).

The DNA sequence of *Csl* showed identity or near identity to numerous mouse, human, rat, and pig ESTs. Using mouse ESTs, primers were designed, and a near full-length cDNA was amplified by reverse transcriptase–PCR from heart RNA, and after cloning multiple isolates were sequenced (Fig. 1 A). BLAST searching revealed that the complete sequence of the human gene spread over five exons was present on two overlapping and fully sequenced cosmid clones derived from the X chromosome (sequence data available from GenBank/EMBL/DDBJ under accession nos. U73508 and U73509; Grieff et al., 1997). Furthermore, the complete rat coding sequence could be assembled from overlapping ESTs. We also isolated and sequenced a *Xenopus laevis* cDNA (Fig. 1 B) and a partial cDNA from zebrafish (Yelon, D., and D. Stainier, unpublished data). However, searches of the *Drosophila melanogaster* and *Caenorhabditis elegans* genomes did not detect *Csl*-related genes. During the course of this study, *Csl* was cloned independently from humans as an X-linked cardiac-expressed gene (Patzak et al., 1999). We determined the chromosomal position of mouse *Csl* by interspecific backcross analysis using a panel of ([C57BL/6J × *Mus spretus*]F1 × C57BL/6J) mice (Copeland and Jenkins, 1991). As in humans (Grieff et al., 1997; Patzak et al., 1999), *Csl* mapped to the X chromosome and was linked to genes *Btk* and *Figf* (data not shown).

Csl proteins were similar in length (85–91 amino acids) with the frog protein being slightly longer than its mammalian counterparts due to the presence of a pentapeptide insertion (Fig. 1 B). Alignments demonstrated strong conservation during vertebrate evolution; mouse Csl is 74% identical to frog Csl and 86 and 92% identical to the human and rat Csl, respectively. No homology was found between Csl and other proteins in public databases.

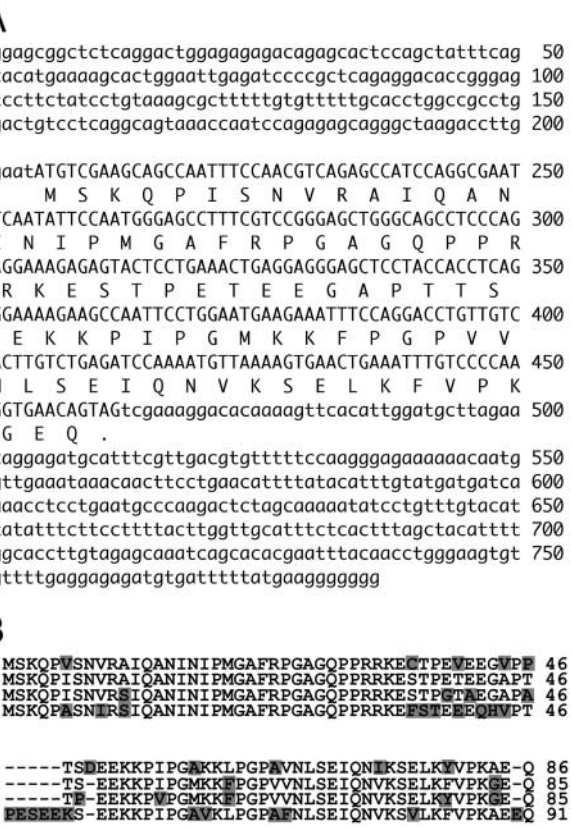

Figure 1. (A) DNA sequence of mouse *Csl* cDNA with predicted protein. (B) Alignment of human, mouse, rat, and *Xenopus* Csl proteins. Shaded amino acids indicate nonidentity. (*Csl* cDNA sequence data available from GenBank/EMBL/DDBJ under accession nos. AY026524 [mouse] and AF343894 [*Xenopus*]).

Csl mRNA Expression in the Embryo and Adult

Most *Csl* ESTs were derived from heart and skeletal muscle. RNase protection analysis of mRNA samples extracted from a variety of adult mouse tissues showed a strong signal in heart, skeletal muscle, and tongue (Fig. 2 A) with a weaker signal in lung, testes, and large intestine. Northern blot analysis of RNA from the C2C12 myogenic cell line revealed a predominant mRNA species of 1.1–1.2 kb (see Fig. 9 A).

Using in situ hybridization, *Csl* transcripts were first detected at E8.25 in myocytes located at the ventral surface of the heart progenitor region undergoing active fusion (Fig. 2, B and C). During the early stages of heart looping (E8–E8.5), *Csl* transcripts were restricted to the myocardial layer at the outer curvature of the presumptive left and right ventricles (Fig. 2, D and E). By E9.5–10.5, transcripts were also evident in the developing sinoatrial region in a left–right asymmetric pattern (Fig. 2, F–I). On the right side, the developing right atrium and right horn of the sinus venosus were strongly positive, whereas on the left a disc-shaped pattern was evident in the dorsolateral region of the common atrium, suggestive of the future position of the left atrial appendage (Fig. 2, G and I). However, the left sinus horn was negative for *Csl* expression. *Csl* expression was undetectable in most of the atrioventricular canal, the inner curvature, and in myocardium associated with the forming atrial septum (Fig. 2, G and I). The outflow tract was also negative, except for a unique rib of expression along its outer curvature (Fig. 2 F). During fetal development, *Csl* expression continued in the outer curvature of the ventricles and in the atrial appendages, as reported in a separate study in which *Csl* was used as an anonymous probe (Christoffels et al., 2000). As expected, *Csl* expression in homozygous *Nkx2-5* mutant embryos was strongly downregulated (Fig. 2 J).

Csl was also expressed in developing skeletal muscles from E11.5. At E13.5, transcripts were evident in the myotomal compartment of somites and in developing limb, head, and neck muscles in a pattern resembling that of the myogenic regulatory factor gene *myogenin* (Fig. 2 K).

Creation of Csl Knockout Mice

To assess the function of *Csl* in muscle development, we generated mutant mice by gene targeting. We designed a

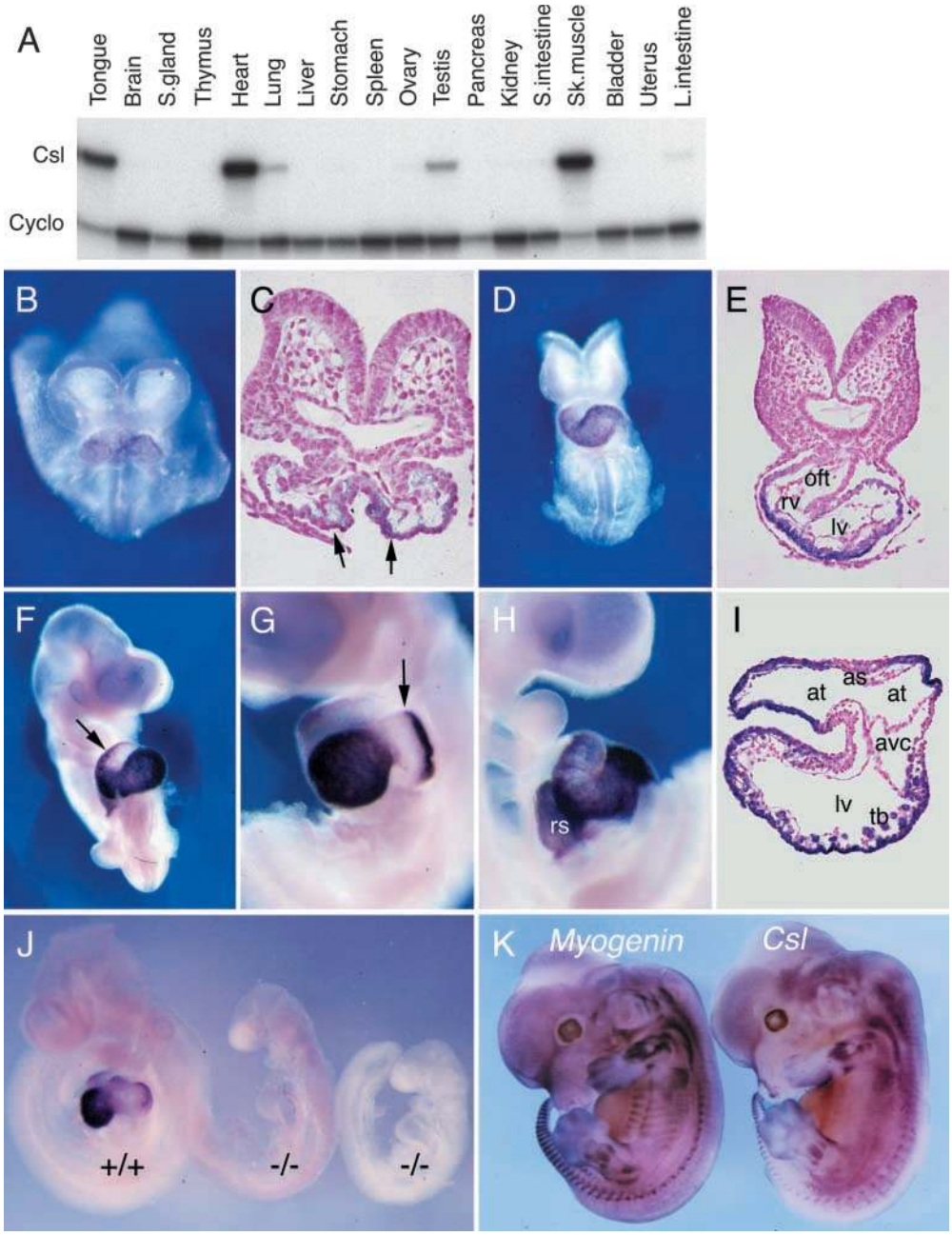

Figure 2. *Csl* mRNA expression. (A) RNase protection analysis of *Csl* and control *cyclophilin* (Cyclo) mRNAs in adult mouse tissues. (B–K) Whole-mount in situ hybridization using *Csl* probe on mouse embryos. (B) Ventral view of E8.25 embryo. (C) Section of the embryo shown in B. Arrows indicate expression on the ventral surface of the fusing heart tube. (D) Ventral view of E8.5 embryo. (E) Section of embryo depicted in D showing *Csl* expression at the outer curvature of the ventricles. (F–H) E10.5 embryo viewed from the ventral and left and right sides, respectively. Arrow in F indicates rib of expression in outflow tract. Arrow in G indicates expression in presumptive left atrial appendage. (I) Section of E10.5 heart. Note that expression is restricted to the outer curvature of the ventricles and atrial appendages. (J) E9.5 *Nkx2-5*$^{-/-}$ embryos (−/−) compared with wild-type sibling (+/+). (K) E13.5 embryos comparing expression of *Csl* and *myogenin*. as, atrial septum; at, atrium; avc, atrioventricular canal; lv, left ventricle; oft, outflow tract; rs, right sinus horn; rv, right ventricle; tb, trabeculae.

conditional targeted allele in which a neomycin resistance cassette was inserted in reverse orientation into the second intron of the *Csl* gene, and Lox P sites were inserted within the untranslated region of the first coding exon (exon 2) upstream of the predicted initiation codon and downstream of the neomycin cassette (Fig. 3 A). A human placental alkaline phosphatase (hPAP) cDNA was also inserted just downstream of the neomycin cassette such that it replaces exon 2 coding sequences after Cre-mediated deletion. The correctly targeted conditional *Csl* allele (Csl^{fAP}) was detected in 1 in 22 (7/153) neomycin-resistant W9.5 embryonic stem cell colonies. Conditional *Csl* lines were established from two independently targeted embryonic stem cell clones, and lines carrying the Cre-deleted allele ($Csl^{APΔ}$) were successfully established after crossing founder chimeras with transgenic mice expressing Cre recombinase in the germline (TgN[CMV-Cre]1Cgn) (Schwenk et al., 1995). Founders were outcrossed onto C57BL/6 mice and progeny were genotyped using PCR (Fig. 3 B). The official designators (Institute for Laboratory Animal Research; http://www4.nas.edu/cls/ilarhome.nsf) for the conditional and Cre-deleted *Csl* mutant strains are Csl^{tm1Rph} and $Csl^{tm1.1Rph}$, respectively.

Western blot analysis of muscle and heart extracts from adult male $Csl^{APΔ}$ mutant mice using an anti-Csl polyclonal antibody revealed no detectable Csl protein (Fig. 4 B), demonstrating that the knockout allele is null. Nevertheless, knockout mice displayed no obvious developmental or structural deficit in heart or skeletal muscle (see Discussion).

Detection of Csl Protein in Muscle and C2C12 Cells

Western blotting revealed a prominent 9-kD band in skeletal muscle and heart (Fig. 4 A), consistent with the pre-

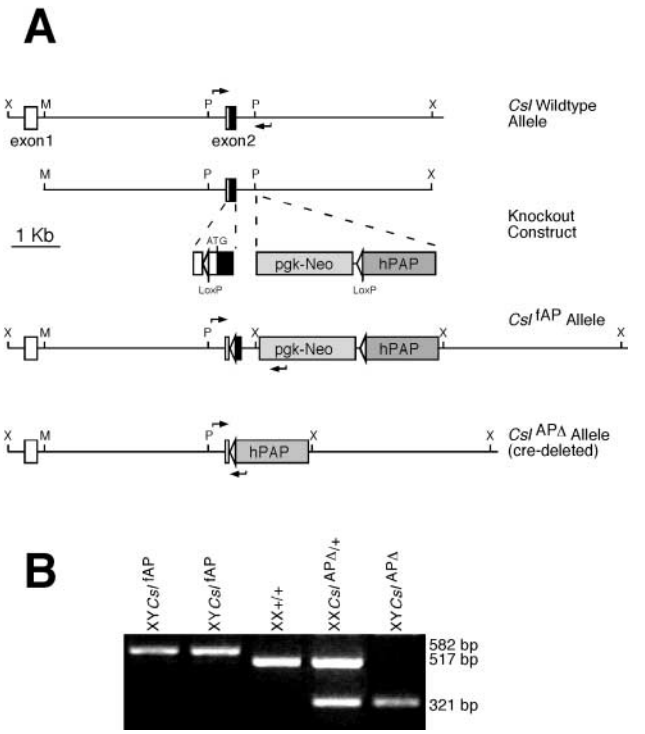

Figure 3. (A) *Csl*-targeting construct relative to wild-type and targeted alleles. Large arrowheads indicate direction of LoxP sites. Black shading within exon 2 indicates *Csl*-coding region. Arrows indicate PCR genotyping primers. hPAP, hPAP gene; pgk-Neo, neomycin resistance gene cassette. (B) Example of multiplex PCR genotyping of targeted (582 bp), wild-type (517 bp), and Cre-deleted (321 bp) alleles. M, MluI; P, PvuII; X, XbaI.

dicted size and distribution of Csl protein. This band was eliminated by prior incubation of antibody with excess recombinant Csl protein (Fig. 4 A). Further analysis showed that the level of Csl protein was higher in muscles of neonatal and postnatal mice (P1–P8) compared with corresponding adult tissues (Fig. 4 B).

Analysis of the mouse C2C12 myogenic cell line (Blau et al., 1983) using immunofluorescence showed that Csl was expressed in differentiating myocytes and myotubes (Fig. 4, D–G), paralleling *Csl* mRNA expression (see Fig. 9 A). Fluorescence was eliminated by prior incubation of antibody with excess recombinant Csl protein (Fig. 4 G). Csl was coexpressed with myofilament proteins in both round and bipolar mononuclear myocytes (Fig. 4, D and E; data not shown), indicating activation at the onset of myogenic differentiation and before fusion. Both native Csl (Fig. 4, D–F) and transfected myc epitope–tagged Csl detected with an anti-myc antibody (data not shown) localized predominantly to the cytoplasm in C2C12 myocytes and myotubes.

Detection of Csl Protein in Adult Tissue Sections

Using immunofluorescence, Csl was robustly expressed in muscles of the heart in all chambers and in skeletal muscles (Fig. 5 A). Analysis of sections of Csl knockout animals revealed only background signal, confirming the specificity of the Csl antibody (Fig. 5 B). Furthermore, staining for hPAP activity in *Csl* knockout mice recapitu-

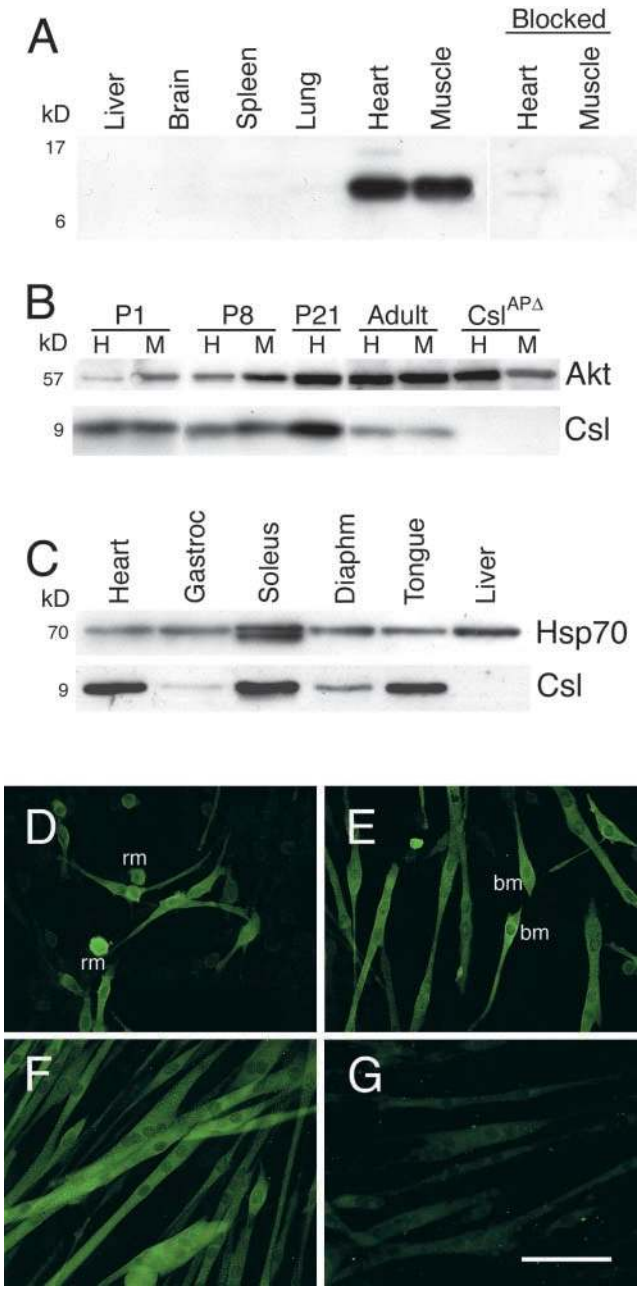

Figure 4. Csl protein expression. (A) Western blot analysis of Csl expression in adult tissues. An equal mass of protein was loaded in each lane. "Blocked" indicates lanes in which Csl antibody was preabsorbed with excess recombinant Csl protein. (B) Western blot analysis of Csl expression in postnatal day (P)1, P8, and P21, and/or adult tissues from wild-type and male $Csl^{AP\Delta}$ knockout mice using Akt levels as loading control. (C) Comparison of levels of Csl expression in heart and different skeletal muscles using Hsp 70 levels as control. Note the additional Hsp 70 isoform enriched in soleus. (D–F) Immunofluorescence analysis of Csl expression in C2C12 cells after 1, 2, and 4 d, respectively, in differentiation medium. (G) Immunofluorescence on 4-d culture after blocking as in A. bm, bipolar mononuclear myocytes; Diaphm, diaphragm; Gastroc, gastrocnemius; rm, rounded mononuclear myocytes. Bar, 100 μm.

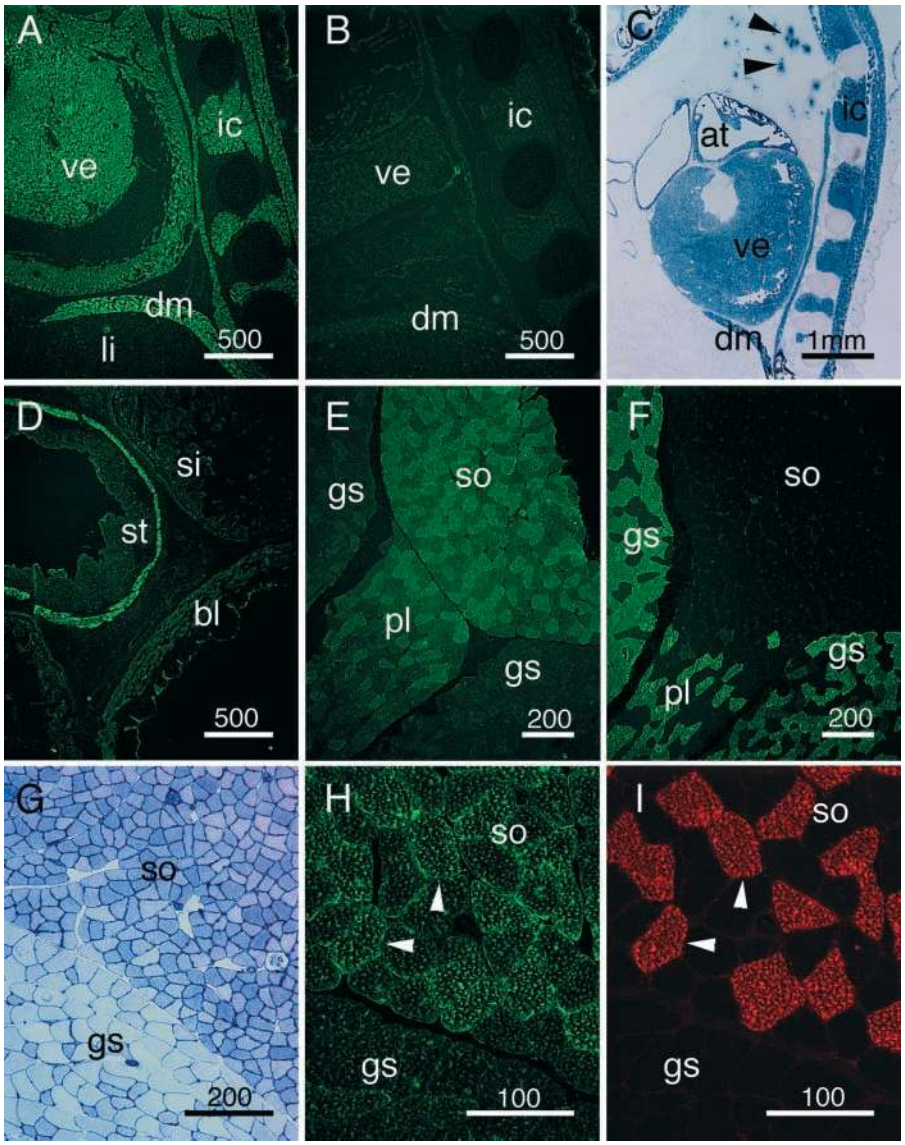

Figure 5. Tissue distribution of Csl protein. Sections from newborn (A–D) and adult (E–I) mice were analyzed for Csl and/or myosin heavy chains using immunofluorescence (A, B, D–F, H, and I) or for Csl by staining for hPAP (C and G). (A) Section showing expression in heart and adjacent skeletal muscles. (B) Section from a $Csl^{AP\Delta}$ mouse. (C) Section from $Csl^{AP\Delta}$ mouse stained for hPAP. Arrowheads show nonspecific staining. (D) Section showing Csl expression in smooth muscle of the stomach. (E and F) Near adjacent sections showing muscle expression of Csl (E) and fast myosin heavy chain IIb (F). (G) Fiber-type pattern of Csl expression in $Csl^{AP\Delta}$ mouse revealed by hPAP staining. (H and I) Double immunofluorescence showing muscle fiber–type pattern of Csl (H) and slow myosin heavy chain I (I). Arrowheads indicate slow fibers showing the highest Csl fluorescence. Bars indicate length in micrometers. at, atrium; bl, bladder; dm, diaphragm; gs, gastrocnemius; ic, intercostal muscle; li, liver; pl, plantaris; si, small intestine; so, soleus; st, stomach; ve, ventricle. Bars: (A, B, and D) 500 μm; (C) 1 μm; (E–G) 200 μm; (H and I) 100 μm.

lated the immunofluorescence patterns (Fig. 5 C). Muscles of the fetal and neonatal stomach were also positive (Fig. 5 D), whereas those of the intestines, bladder, and vasculature were negative. Smooth muscles surrounding pulmonary veins, which are cardiac in character (Millino et al., 2000), also expressed Csl (data not shown), presumably accounting for the RNase protection signal in lungs (Fig. 2 A). Stomach expression was transient, since RNase protection analysis (Fig. 2 A) and immunofluorescence (data not shown) failed to detect Csl transcript or protein in adults. *Csl* mRNA was also expressed in testes (Fig. 2 A), and in knockout mice the germ cell component was hPAP positive. However, no Csl protein could be detected in these cells (data not shown).

In adult skeletal muscles, the level of Csl protein varied considerably between muscles with different metabolic and functional characteristics. Western blotting showed that Csl levels were highest in slow oxidative muscles, such as the soleus, and lowest in fast glycolytic muscles, such as the gastrocnemius (Fig. 4 C), with intermediate levels in tongue and diaphragm. This pattern was also evident using immunofluorescence (Fig. 5, E and H) and in *Csl* knockout mice by hPAP staining (Fig. 5 G). Double immunofluorescence with antibodies against fiber type–specific myosin heavy chains revealed that the level of Csl protein was in fact graded within individual muscle fibers, with highest levels in slow type I, intermediate levels in fast type IIa, and lowest levels in fast type IIb fibers (Fig. 5, E, F, H, and I; data not shown).

Intracellular Distribution of Csl Protein

In cardiac and skeletal muscles of the fetus, Csl protein was localized relatively evenly throughout the cell, even in the presence of clearly organized sarcomeres, revealed by double immunofluorescence with α-actinin antibody (Fig. 6, A and B). However, a striated pattern of Csl immunolocalization became evident from late fetal to neonatal stages and was the predominant pattern in the adult (Fig. 6, D and J). Confocal microscopic analysis of stretched slow adult skeletal muscles (soleus) revealed that Csl was expressed predominantly in repetitive double stripes (Fig. 6, D and G). Doublets localized to the level of the I-band,

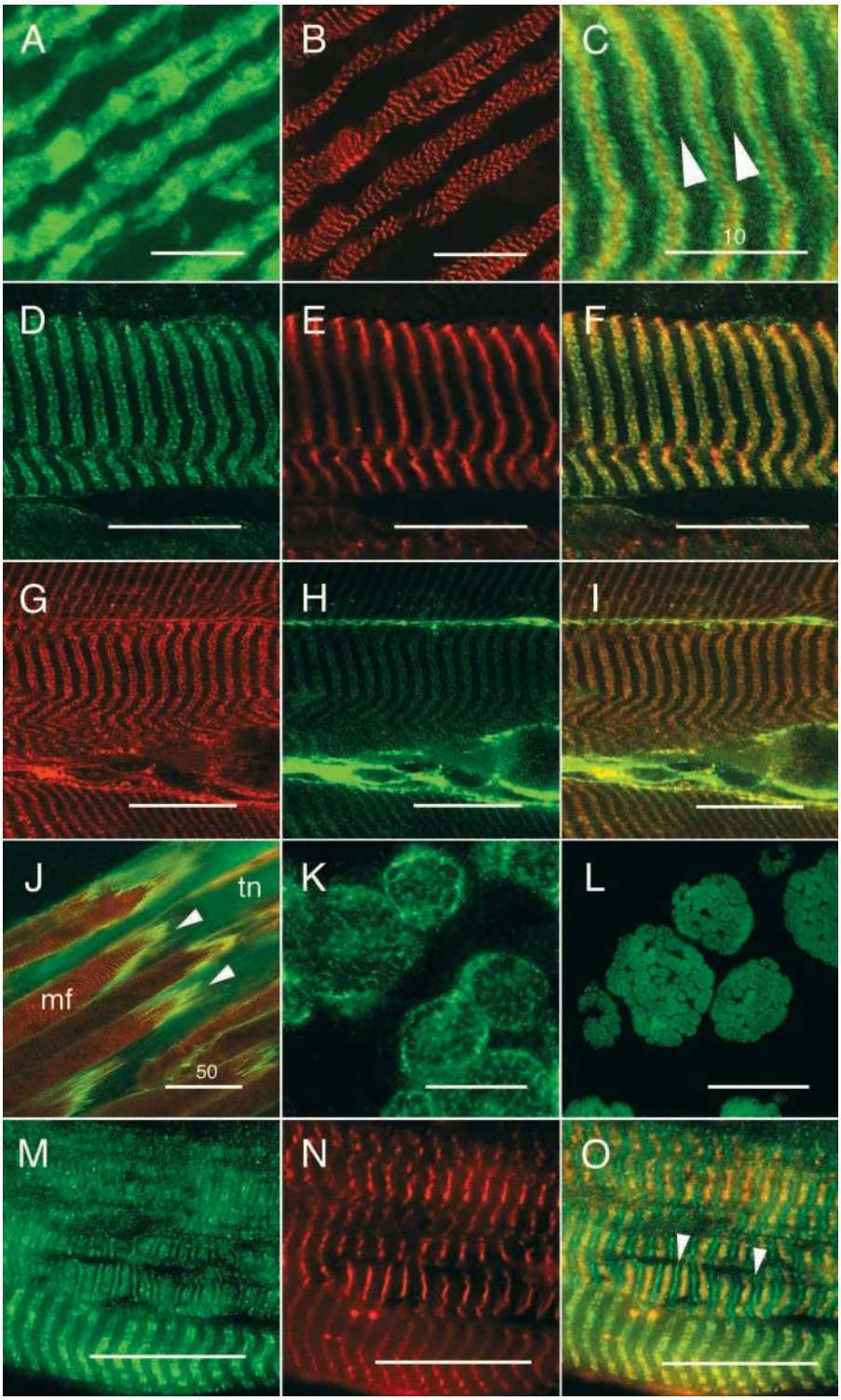

Figure 6. Subcellular localization of Csl protein. (A and B) Double immunofluorescence on a section of E18.5 skeletal muscle showing localization of Csl (A) and α-actinin (B). (C) High power double immunofluorescence confocal image (overlay) of a section of stretched adult soleus (see D–F) showing Csl (green) and α-actinin (red). Arrowheads indicate weak Csl staining over the M-line. (D–F) Double immunofluorescence confocal image of a section of stretched adult soleus showing Csl (D), α-actinin (E), and overlay (F). (G–I) Confocal images of Csl (G) and talin (H) with overlay (I). (J) Overlay of Csl and talin double immunofluorescence in myotendenous junctions (arrowheads). (K and L) Transverse sections of E17.5 myotubes showing Csl (K) and α-actinin (L). (M–O) Double immunofluorescence of Csl (M) and α-actinin (N) with overlay (O) in adult ventricular myocytes. Arrowheads indicate Csl staining over the M-line. mf, myofiber; tn, tendon. Bars: (A, B, D–I, and K–L) 20 μm; (C) 10 μm; (J) 50 μm.

flanking the Z-line, the point of attachment of actin thin filaments of adjacent sarcomeres seen as a single line of α-actinin in double immunofluorescence (Fig. 6, D–F). This pattern suggests localization to costameres, subsarcolemmal sites of cytoskeletal/membrane adhesion complexes (Pardo et al., 1983; Berthier and Blaineau, 1997). Indeed, Csl colocalized with talin (Fig. 6, G–I), a large protein with actin-, vinculin-, integrin-, and dystrophin-binding activities enriched in a variety of matrix–cytoskeleton adhesive complexes, including costameres (Berthier and Blaineau, 1997). A weak single stripe of Csl expression was also seen between the strong doublets at the level of the M-line (Fig. 6 C). Unlike α-actinin, which is located throughout the myofibril at the level of the Z-line (Fig. 6 L), Csl was present predominantly surrounding or between myofibrils (Fig. 6 K). The honeycomb-like pattern of Csl in transverse sections of fetal myotubes resembled that of the intermediate filament protein desmin, which precisely sur-

rounds the Z-line of myofibrils in a cage-like manner in continuity with costameres at the membrane (Granger and Lazarides, 1979). Csl also colocalized with talin in myotendonous junctions (Fig. 6 J).

The Csl pattern in adult cardiac muscles appeared identical to that found in the soleus (Fig. 6, M–O), although the smaller size of the cardiac cells made individual bands more difficult to resolve. Nevertheless, doublets flanking the Z-line and an association with the M-line were evident. The M-line signal was more prominent than in skeletal muscles (Fig. 6 C).

Dominant Effects of Csl in C2C12 Cells

We overexpressed Csl in the C2C12 myogenic cell line (Blau et al., 1983) and examined effects on myoblasts and myocyte formation in the presence and absence of insulin-like growth factor (IGF)-1, a known proliferative, viability, promyogenic, hypertrophic, and repair factor for muscle cells (Coolican et al., 1997; Gredinger et al., 1998; Goldspink, 1999; Musaro and Rosenthal, 1999; Musaro et al., 1999; Semsarian et al., 1999; Lawlor and Rotwein, 2000). Prior studies in the rat L6E9 line demonstrated that enforced Csl expression induced formation of large hypertrophied myotubes after 2 d of differentiation in the presence of IGF-1 (Musaro, A., and N. Rosenthal, personal communication). In this study, C2C12 lines stably expressing FLAG-Csl under control of the EF1α promoter were analyzed in detail.

Dominant effects of ectopic FLAG-Csl were first seen at the myoblast stage. In the FC18 Csl-expressing line, myoblasts appeared larger than the F5 vector–only control line due to induction of prominent lamellipodia accompanied by membrane ruffling. To ensure that this was not due to clonal variation or the nature of the epitope tag, we generated further stable lines expressing myc epitope–tagged Csl under control of the EF1α promoter and the myosin light chain-1F promoter/3′ enhancer (MLC1), the latter expressed in myocytes but not in myoblasts (Musaro and Rosenthal, 1999). An additional control line expressed green fluorescent protein (GFP) under cytomegalovirus promoter control. These new lines were established in a different clonal isolate of C2C12 that underwent more rapid differentiation in low serum (see Materials and Methods). EF1α-myc-Csl lines but not parental or control lines showed prominent lamellipodia (Fig. 7, A and B). To quantify the effects, we measured mean cell area using planimetry. Myc-Csl– and FLAG-Csl–expressing myoblasts showed a significant increase in area (Fig. 7 C), most pronounced in the myc-Csl lines ME1 and ME2. The myc-Csl lines MM1 and MM2, which do not express Csl in myoblasts, were the same size as those carrying GFP vector–only or untransfected controls. This effect was due solely to cell spreading on the tissue culture dish, since flow cytometry using forward light scatter showed that the volume of detached Csl-myoblasts was no different from that of controls (Fig. 7, D and E). Immunofluorescence of myc-Csl–expressing myoblasts revealed that a proportion of Csl protein became localized to membrane ruffles at the leading edge of lamellipodia (Fig. 7 G) and to focal adhesions (not shown). Membrane ruffle localization of a fusion protein consisting of GFP linked in frame to the NH_2 terminus of Csl was also evident after expression in myoblasts (Fig. 7

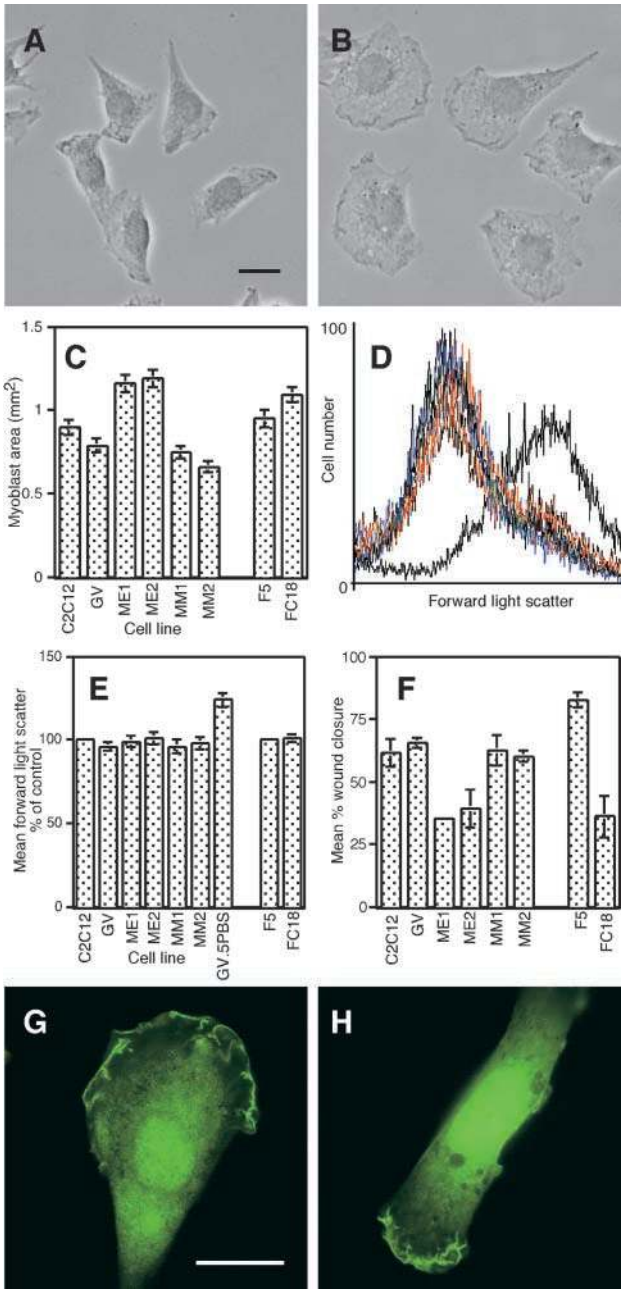

Figure 7. Effect of constitutive Csl expression in C2C12 myoblasts. (A and B) Phase–contrast images of stable C2C12 clones constitutively expressing GFP (A) or myc-Csl (B). (C) Mean myoblast area (± SEM) of parental C2C12 cells and a series of transfected myc- or FLAG-Csl–expressing clones. GV is transfected with GFP vector only; ME1/2 are lines expressing myc-Csl driven by EF1α promoter; MM1/2 are lines expressing myc-Csl driven by differentiation-dependent MLC1 promoter/enhancer. Only ME1, ME2, and FC18 express Csl in myoblasts. (D) Overlay of forward light scatter histograms from a single experiment in which C2C12 stable clones (GV, ME1, ME2, MM1, MM2) and parental cell line were compared. As positive control, GV cells were resuspended in hypotonic 0.5× PBS causing a rightward shift. (E) Mean forward light scatter (± SEM) determined from three separate experiments and plotted as a percentage of controls. (F) Mean percentage (± SEM) of closure of 150-μm wounds in confluent monolayers after 6 h. (G) Anti-myc antibody immunofluorescence in a myc-Csl–expressing myoblast. (H) GFP fluorescence in a C2C12 myoblast transiently expressing GFP–Csl fusion protein. Bars, 20 μm.

H). Despite their prominent lamellipodia, Csl-expressing myoblasts migrated more slowly than controls in a cell monolayer wound repair migration assay (Fig. 7 F).

Csl Induces Myosacs in C2C12 Cells in an IGF-1–dependent Fashion

After transfer to low serum medium, FLAG-Csl cells were delayed in the onset of myotube formation by 12–24 h, seen also as a delay in the onset of expression of the bHLH factor myogenin and the cyclin/cdk inhibitor $p21^{WAF1/Cip1}$ (data not shown). Nevertheless, differentiation into long thin myotubes occurred relatively normally (Fig. 8, A and B). We therefore assessed the outcome of adding recombinant human IGF-1 to differentiating cultures. The effects of IGF-1 on muscle cells are dose dependent, and at the high concentration used in these experiments (100 ng/ml; 13 nM) proliferation is the favored response (Coolican et al., 1997; Layne and Farmer, 1999). Thus, IGF-1 added to control cultures from the beginning of differentiation induced an extended period of myoblast proliferation and a higher density of cells in differentiating cultures but no obvious hypertrophy (Fig. 8 C). However, addition of IGF-1 to FLAG-Csl cells induced formation of massively hypertrophied myotubes throughout the culture after 3 d of differentiation (Fig. 8 D). These cells, dubbed "myosacs" (Yotov and St-Arnaud, 1996), were highly branched and contained many nuclei. They resembled myotubes induced in L6E9 and related muscle cell lines by IGF-1 (Coolican et al., 1997; Musaro et al., 1999) and in C2 cells by a variety of stimuli, including treatments that enhance cell fusion (Yagami-Hiromasa et al., 1995; Hirayama et al., 1999). All three FLAG-Csl lines examined exhibited the same phenotype, although myosacs were not observed in any of the myc-Csl lines (see Discussion). Although myosacs were highly dysmorphogenic, immunostaining revealed no obvious mislocalization of myosin heavy chains, actin, tubulin, or α-actinin (Fig. 8, G and H; data not shown).

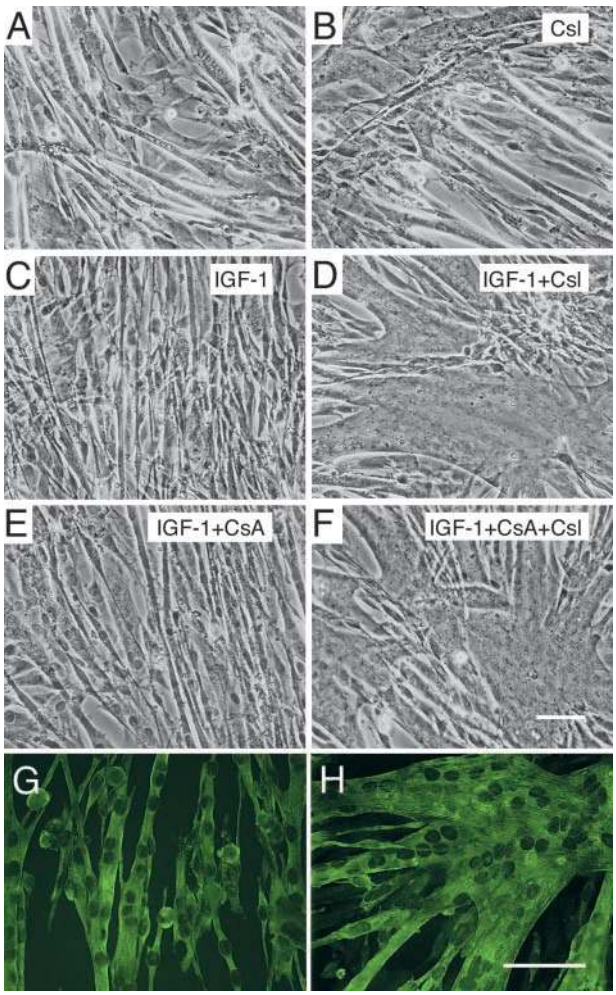

Figure 8. Effects of constitutive FLAG-Csl expression in differentiating C2C12 myogenic cells. Phase–contrast and immunofluorescence images of control (F5; left panels) and FLAG-Csl–expressing (FC18; right panels) C2C12 cells after 3 d of differentiation. (A and B) No treatment. (C and D) With 100 ng/ml IGF-1. (E and F) With 100 ng/ml IGF-1 plus 1 μM CsA. (G and H) MF20 immunofluorescence on cells treated with IGF-1. Bars, 100 μm.

Csl Augments the Activity of NFAT and MEF2 Transcription Factors in the Presence of IGF-1

To determine whether myosac formation reflected increased myogenesis, we assayed the expression of several muscle genes in FC18 and F5 cultures using Northern blotting (Fig. 9 A). No significant effects on mRNAs for myogenin, MEF2C, and embryonic myosin heavy chain were discernible either in the presence or absence of IGF-1. Analysis of protein to DNA ratios in differentiating cultures (Fig. 9 B) showed that the myosac phenotype was not the result of increased anabolic metabolism (increased protein synthesis relative to DNA synthesis), a component of skeletal muscle hypertrophy (Goldspink, 1999). Indeed, Csl actually decreased protein to DNA ratios at late times in the culture, independently of IGF-1. We also measured the activities of transfected reporter genes dependent on the transcription factors NFAT and MEF2, both of which are known to be important for skeletal muscle differentiation and hypertrophy (Abbott et al., 1998; Wu et al., 2000). In control cultures, the activities of NFAT (assayed on a 2-kb *myoglobin* promoter relative to a mutant version lacking NFAT sites [Chin et al., 1998]) and MEF2 (assayed on three MEF2-binding sites juxtaposed to a minimal promoter relative to minimal promoter only [Chen et al., 2000]) were low at early stages of differentiation but increased progressively to day 4 (Fig. 10, A–D). Although IGF-1 elevated levels of MEF2 and to a lesser extent NFAT (Fig. 10, B and D), FLAG-Csl in the presence of IGF-1 induced a significant further increase in both NFAT and MEF2 activity after 3 d (Fig. 10, B and D). The NFAT effect was seen in all three FLAG-Csl lines analyzed. NFAT and MEF2 are targets of the Ca^{2+}/calcineurin signaling pathway (Abbott et al., 1998; Chin et al., 1998; Molkentin et al., 1998; Semsarian et al., 1999; Delling et al., 2000; Wu et al., 2000). However, we found that the Csl/IGF-1–mediated increase in NFAT activity was largely resistant to the calcineurin inhibitory drug CsA (1 μM) (Fig. 10 F). CsA at this dose effectively blocked calcineurin activity, since it completely inhibited the increase in NFAT activity conferred by transient expression of a constitutively active calcineurin variant at day 4 (Chin et al., 1998)

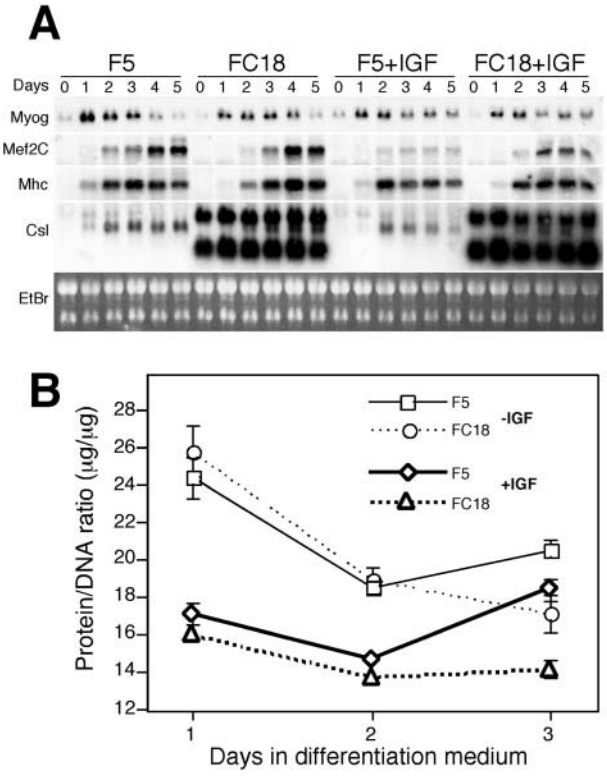

Figure 9. Myogenic gene expression and protein to DNA ratios in control (F5) and FLAG-Csl (FC18) C2C12 cells in the presence and absence of IGF-1 (100 ng/ml). (A) Northern blot analysis of total RNA from cells cultured for 0–5 d in differentiation medium using indicated probes. Ethidium bromide (EtBr) staining of 28S and 18S ribosomal RNAs serves as loading control. Two mRNA species are produced from the transgene due to differential 3′ untranlated region processing. (B) Total protein/total DNA ratios ± SEM at different times of differentiation. Myog, *myogenin*; Mhc, *embryonic myosin heavy chain*.

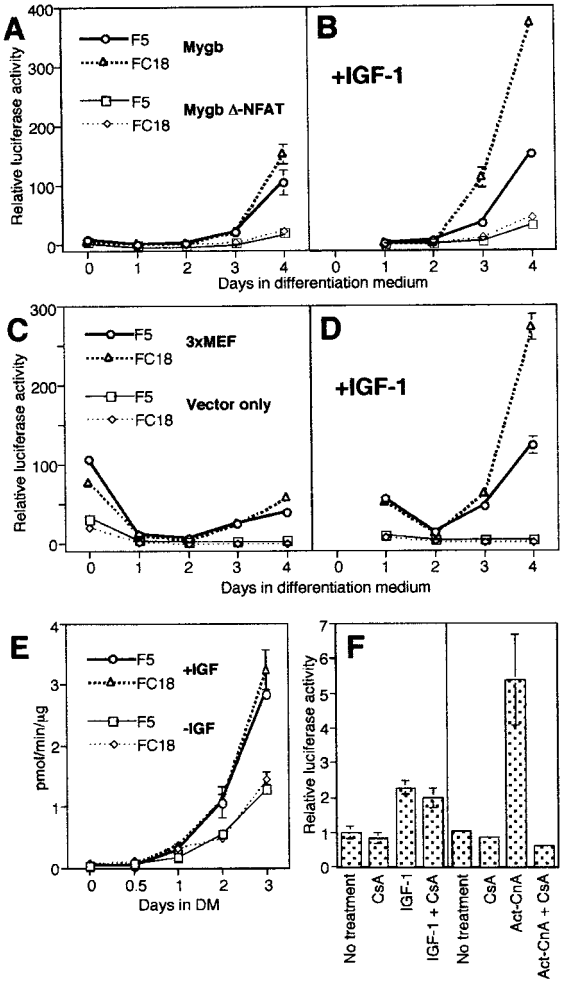

Figure 10. NFAT, MEF2, and calcineurin activity in control (F5) and FLAG-Csl (FC18) cells with and without IGF-1 (100 ng/ml). (A and B) Mean NFAT-dependent transcriptional activity (± SEM) measured using a transfected luciferase reporter gene driven by the *myoglobin* promoter (Mygb), compared with the same promoter with mutated NFAT-binding sites (Mygb Δ-NFAT). (C and D) Mean MEF2-dependent transcriptional activity (± SEM) measured using a transfected luciferase reporter containing three MEF2-binding sites (3×MEF) compared with the minimal vector (Vector only). (E) Levels of calcineurin phosphatase activity measured in vitro as picomoles of ^{32}P-radiolabeled phosphate released per minute per microgram of extract (pmol/min/μg). (F) Effect of CsA (1 μM) on NFAT activity measured using the wild-type *myoglobin* (Mygb) reporter at day 4 in FC18 cells after treatment with IGF-1 (left) or after transient transfection of activated calcineurin A subunit (Act-CnA) (right).

(Fig. 10 F). In the C2C12 subline used in these experiments (see Materials and Methods), calcineurin activity assayed in extracts was low at early stages of the culture but increased with further differentiation (Fig. 10 E). Activity was stimulated by the presence of IGF-1 as demonstrated previously (Semsarian et al., 1999), although there was no further increase with FLAG-Csl (Fig. 10 E). In contrast to primary muscle cultures and other cell lines (Musaro et al., 1999; Delling et al., 2000; Friday et al., 2000), differentiation in this line appeared totally resistant to CsA added either at the beginning of differentiation or up to 3 h beforehand (Fig. 8 E). This fact has allowed us to uniquely assess whether myosac formation was resistant to CsA, uncomplicated by effects of the drug on differentiation. However, myosac formation was totally insensitive to CsA (Fig. 8, E and F).

Discussion

We have cloned a cDNA encoding the 9-kD muscle-specific protein Csl in a screen for novel transcriptional targets of the cardiac homeodomain factor Nkx2-5 (Harvey, 1996). In embryonic hearts, *Csl* was expressed exclusively at the outer curvature of the ventricles and in the atrial appendages but not at the inner curvature. The *Csl*-positive domains appear to define regions that will form the working myocardium of the heart chambers, which are specified at the outer curvature in response to anterior/posterior and dorsal/ventral patterning information (Christoffels et al., 2000). Indeed, *Csl* is one of few markers that highlight the primordia of chamber myocardium in very early hearts. The pattern of *Csl* expression in the sinoatrial region of the heart is also noteworthy in light of its complex development and lineage contributions (Anderson et al., 1999). *Csl* transcripts were seen in the developing right atrial ap-

pendage and right sinus horn, the latter becoming incorporated into the right atrium as development proceeds (Anderson et al., 1999). However, the left sinus horn did not express detectable levels of *Csl* at early times. This horn is not substantially incorporated into the atrium, but retains its original walls to form in humans the coronary sinus and in the mouse the persistent connection to the left superior vena cava. The above findings suggest that myocytes forming the working component of heart chambers undergo transition to a more specialized myogenic phenotype via a distinct Nkx2-5–dependent genetic program.

Using a polyclonal antibody, we detected Csl protein in the heart, all skeletal muscles, and smooth muscles of the stomach and lungs, and this distribution was confirmed by staining for hPAP in *Csl* knockout mice. The intracellular localization of Csl protein was complex. In embryonic and fetal cardiac and skeletal muscles and in C2C12 myotubes, Csl was present throughout the cytoplasm of the cell, even in the presence of well-formed myofilamentous structures. However, Csl became associated with the sarcomeric cytoskeleton as myofibers matured. This was predominantly in a costameric pattern. Costameres are discrete, rectilinear, subsarcolemmal domains that appear as transverse stripes along the muscle fiber (Pardo et al., 1983; Berthier and Blaineau, 1997) originally defined by the expression pattern of vinculin, which aligns with I-band regions of the sarcomere flanking the Z-lines. Costameres contain supramolecular complexes of focal adhesion–type, spectrin-based, and dystrophin-based cytoskeletal membrane adhesion systems that are thought to stabilize the sarcolemma of muscle cells by distributing force to the extracellular matrix during contractions (Berthier and Blaineau, 1997). Many of the proteins that localize to or are enriched in costameres are also found in myotendonous and neuromuscular junctions in muscle cells and in focal adhesions and membrane ruffles in nonmuscle cells (Berthier and Blaineau, 1997; Brancaccio et al., 1999). In addition to their mechanical functions, the above structures tether many signaling molecules, which control mechanoreception, cytoskeletal remodelling, and other myogenic functions in response to internal and external stimuli (Berthier and Blaineau, 1997; Goldspink, 1999). The pattern of Csl immunofluorescence in skeletal muscle cells suggests that Csl is localized both within subsarcolemmal costameres and intracellularly in paired rings flanking the Z-lines of myofibrils seen typically as a honeycomb pattern in transverse sections. A lower level of Csl protein was also seen between the I-band doublets overlying the M-line, showing that Csl is not localized exclusively to the costameric lattice. Levels of Csl protein also showed a distinct fiber-type bias in skeletal muscle cells, suggesting modulation by neuronal input and/or load (Goldspink, 1999). In cardiocytes, the Csl pattern appeared essentially identical to that in slow skeletal muscle. These complex distributions hint at functions (perhaps multiple) in cytoskeletal/myofilament organization and regulation and/or associated signaling.

We have approached the function of *Csl* by gene knockout and overexpression experiments. The conditional knockout allele of *Csl*, which appears to be null, showed no overt developmental phenotype in skeletal muscle or heart, suggesting genetic or functional redundancy and/or a dedicated role in muscle adaptation and regeneration. Analysis of responses to stress, injury, and aging in muscles of knockout mice is underway. Overexpression of Csl in C2C12 myogenic cells induced several dominant effects. In myoblasts, ectopic Csl induced lamellipodia, and Csl protein became localized to leading edge membrane ruffles and focal adhesions. It is well established that cell division and changes in cell shape and behavior, including formation of lamellipodia and membrane ruffling during cell migration, are mediated by actomyosin cytoskeletal dynamics and require the Rho family of small GTPases (Kaibuchi et al., 1999; Bishop and Hall, 2000). Formation of lamellipodia seems to be mediated predominantly by Rac1 and stress fibers, and focal adhesion by Rho (Nobes and Hall, 1995). These findings suggest that ectopically expressed Csl may engage up- or downstream elements of Rho/Rac-signaling cascades and thus dysregulate actomyosin dynamics. Paradoxically, Csl-expressing cells could not efficiently migrate into cell monolayer wounds. In addition to inducing lamellipodia, Csl may stabilize trailing edge focal adhesions, which normally must disassemble during migration. Whether the effects relate to the normal role of Csl must remain highly speculative at this point, since Csl is not normally expressed in myoblasts. However, there is an intriguing connection between the dominant functions of Csl in myoblasts and its localization to costameres in normal muscle cells, which share many features of other actin membrane adhesion systems such as lamellipodia (Berthier and Blaineau, 1997).

During differentiation of C2C12 cells in low serum, Csl overexpression induced formation of large dysmorphogenic myosacs in an IGF-1 signaling–dependent manner. This phenotype did not appear to be due to augmented myogenesis nor was it accompanied by an increase in anabolic metabolism, a component of skeletal muscle hypertrophy. Furthermore, myosac formation was CsA insensitive and therefore independent of the Ca^{2+}/calmodulin–dependent phosphatase calcineurin (Rusnak and Mertz, 2000) implicated in skeletal muscle hypertrophy in vitro and in vivo (Dunn et al., 1999; Musaro et al., 1999; Semsarian et al., 1999). Since Csl-induced myosacs contained large numbers of nuclei, we favor the hypothesis that in the C2C12 line, myosacs form through augmentation and dysregulation of myocyte fusion. Myocyte fusion occurs in a complex and highly orchestrated progression involving cell recognition, adhesion, alignment, and membrane fusion (Doberstein et al., 1997; Hirayama et al., 1999). Importantly, induction of promiscuous fusion in C2 cells with Sendai virus or metalloprotease disintegrin overexpression induces a myosac-like phenotype (Yagami-Hiromasa et al., 1995; Hirayama et al., 1999), and expression of dominant negative forms of Rac1 in *Drosophila* muscle precursors induces promiscuous fusion and formation of myosac-like muscles in situ (Luo et al., 1994). Thus, it is possible that the two dominant effects of overexpressed Csl discussed above share a common mechanism, that is, perturbation of regulated cytoskeletal dynamics. However, Myc-Csl overexpression did not induce myosacs in a subline of C2C12 cells that differentiate 1–2 d in advance of those in which myosacs were observed. Although the reason for this is unclear, it is possible that the rat L6E9 line in which the myosac phenotype was initially observed and the permissive C2C12 line have become less robust with respect

to regulation of cytoskeletal remodelling due to adaptations to tissue culture.

In addition to its dominant effects on myoblast and myocyte cell shape and behavior, Csl also augmented the activities of the NFAT and MEF2 families of transcription factors in an IGF-1 signaling–dependent manner at late stages in the culture. For NFAT, this effect was largely CsA insensitive, indicating that it did not involve the calcineurin pathway. The mechanism of this augmentation is unknown, although it highlights the fact that overexpression of Csl can influence intracellular signaling events in addition to structural changes. Since both NFAT and MEF2 regulate the myoglobin promoter, which is selectively expressed in slow fibers (Chin et al., 1998), and since Csl itself is enriched in slow fibers, overexpression of Csl in C2C12 cells may promote a slow fiber phenotype. It is also possible that the activity of NFAT and MEF2 like that of serum response factor, a key transcriptional regulator in muscle cells, is stimulated by increased actin dynamics (Sotiropoulos et al., 1999). Although we acknowledge that overexpression experiments require cautious interpretation, further analysis of the above effects may offer new insights into Csl function in muscle cells and the prominent role played by the cytoskeleton and myofilament and its associated signaling molecules in muscle development, function, and disease.

We thank Nadia Rosenthal for sharing initial findings in L6E9 cells and for critical input. We thank Bob Graham, Ming-Jie Wu, and Peter Riek for advice; Eva Chin, David Huang, George Muscat, and Sanders Williams for plasmids; Debra Gilbert for technical assistance; Edna Hardeman for antibodies and cell lines; and Mark Solloway and Anne Cunningham for confocal microscope expertise.

This work was supported by the National Health and Medical Research Council, Australia (9937381), the National Institutes of Health National Institute of Aging (RO3 AG14811), and the National Cancer Institute (Department of Health and Human Services). S. Palmer held a Wellcome Trust Travelling Research Fellowship; A. Schindeler held an Australian Postgraduate Award; and T. Yeoh held an NHMRC Postgraduate Medical Scholarship.

Submitted: 2 February 2001
Revised: 5 April 2001
Accepted: 11 April 2001

Note added in proof: Csl (*Smpx*) was recently cloned as a gene responsive to stretch in skeletal muscle cells (Kemp, T.J., T.J. Sadusky, M. Simon, R. Brown, M. Eastwood, D.A. Sassoon, and G.R. Coulton. 2001. Identification of a novel stretch-responsive skeletal muscle gene [*Smpx*]. *Genomics.* 72:260–271).

References

Abbott, K.L., B.B. Friday, D. Thaloor, T.J. Murphy, and G.K. Pavlath. 1998. Activation and cellular localization of the cyclosporine A-sensitive transcription factor NF-AT in skeletal muscle. *Mol. Biol. Chem.* 9:2905–2916.

Anderson, R.H., S. Webb, and N.A. Brown. 1999. Clinical anatomy of the atrial septum with reference to its developmental components. *Clin. Anat.* 12:362–374.

Berthier, C., and S. Blaineau. 1997. Supramolecular organization of the subsarcolemmal cytoskeleton of adult muscle fibers. A review. *Biol. Cell*. 89:413–434.

Biben, C., and R.P. Harvey. 1997. Homeodomain factor Nkx2-5 controls left-right asymmetric expression of bHLH *eHand* during murine heart development. *Genes Dev.* 11:1357–1369.

Biben, C., D.A. Palmer, D.A. Elliot, and R.P. Harvey. 1997. Homeobox genes and heart development. *Cold Spring Harb. Symp. Quant. Biol.* 62:395–403.

Biben, C., R. Weber, S. Kesteven, E. Stanley, L. McDonald, D.A. Elliott, L. Barnett, F. Koentgen, L. Robb, M. Feneley, et al. 2000. Cardiac septal and valvular dysmorphogenesis in mice heterozygous for mutations in the homeobox gene *Nkx2-5*. *Circ. Res.* 87:888–895.

Bishop, A.L., and A. Hall. 2000. Rho GTPases and their effector proteins. *Biochem. J.* 348:241–255.

Blau, H., C.-P. Chiu, and C. Webster. 1983. Cytoplasmic activation of human nuclear genes in stable heterocaryons. *Cell*. 32:1171–1180.

Brancaccio, M., S. Guazzone, N. Menini, E. Sibona, E. Hirsch, M. De Andrea, M. Rocchi, F. Altruda, G. Tarone, and L. Silengo. 1999. Melusin is a new muscle-specific interactor for β_1 integrin cytoplasmic domain. *J. Cell Biol.* 274:29282–29288.

Bruneau, B.G., Z.-Z. Bao, M. Tanaka, J.-J. Schott, S. Izumo, C.L. Cepko, J.G. Seidman, and C.E. Seidman. 2000. Cardiac expression of the ventricle-specific homeobox gene *Irx4* is modulated by Nkx2-5 and dHand. *Dev. Biol.* 217:266–277.

Chen, C.Y., and R.J. Schwartz. 1996. Recruitment of the tinman homologue Nkx-2.5 by serum response factor activates cardiac α-actin gene transcription. *Mol. Cell. Biol.* 16:6372–6384.

Chen, S.L., D.H. Dowhan, B.M. Hosking, and G.E.O. Muscat. 2000. The steroid receptor coactivator, GRIP-1, is necessary for MEF2C dependent gene expression and skeletal muscle differentiation. *Genes Dev.* 14:1209–1228.

Chin, E.R., E.N. Olson, J.A. Richardson, Q. Yang, C. Humphries, J.M. Shelton, H. Wu, W. Zhu, R. Bassel-Duby, and R.S. Williams. 1998. A calcineurin-dependent transcriptional pathway controls skeletal muscle fiber type. *Genes Dev.* 12:2499–2509.

Christoffels, V.M., P.E.M.H. Habets, D. Franco, M. Campione, F. de Jong, W.H. Lamers, Z.-Z. Bao, S. Palmer, C. Biben, R.P. Harvey, and F.M. Moorman. 2000. Chamber formation and morphogenesis in the developing mammalian heart. *Dev. Biol.* 223:266–278.

Cleaver, O.B., K.D. Patterson, and P.A. Krieg. 1996. Overexpression of the *tinman*-related genes *XNkx-2.5* and *XNkx-2.3* in *Xenopus* embryos results in myocardial hyperplasia. *Development*. 122:3549–3556.

Coolican, S.A., D.S. Samuel, D.Z. Ewton, F.J. McWade, and J.R. Florini. 1997. The mitogenic and myogenic actions of insulin-like growth factors utilize distinct signaling pathways. *J. Biol. Chem.* 272:6653–6662.

Copeland, N.G., and N.A. Jenkins. 1991. Development and applications of a molecular genetic linkage map of the mouse genome. *Trends Genet.* 7:113–118.

Delling, U., J. Tureckova, H.W. Lim, L.J. De Windt, R. Rotwein, and J.D. Molkentin. 2000. A calcineurin-NFATc3-dependent pathway regulates skeletal muscle differentiation and slow myosin heavy-chain expression. *Mol. Cell. Biol.* 20:6600–6611.

Doberstein, S.K., R.D. Fetter, A.Y. Mehta, and C.S. Goodman. 1997. Genetic analysis of myoblast fusion: *blown fuse* is required for progression beyond the prefusion complex. *J. Cell Biol.* 136:1249–1261.

Dunn, S.E., J.L. Burns, and R.N. Michel. 1999. Calcineurin is required for skeletal muscle hypertrophy. *J. Biol. Chem.* 274:21908–21912.

Durocher, D., C.-Y. Chen, A. Ardati, R.J. Schwartz, and M. Nemer. 1996. The atrial natriuretic factor promoter is a downstream target for Nkx-2.5 in the myocardium. *Mol. Cell. Biol.* 16:4648–4655.

Durocher, D., F. Charron, R. Warren, R.J. Schwartz, and M. Nemer. 1997. The cardiac transcription factors Nkx2-5 and GATA-4 are mutual cofactors. *EMBO J.* 16:5687–5696.

Fishman, M.C., and K.R. Chien. 1997. Fashioning the vertebrate heart: earliest embryonic decisions. *Development*. 124:2099–2117.

Friday, B.B., V. Horsley, and G.K. Pavlath. 2000. Calcineurin activity is required for the initiation of skeletal muscle differentiation. *J. Cell Biol.* 149: 657–665.

Fu, Y., W. Yan, T.J. Mohun, and S.M. Evans. 1998. Vertebrate *tinman* homologues *XNkx2-3* and X*Nkx2-5* are required for heart formation in a functionally redundant manner. *Development*. 125:4439–4449.

Goldspink, G. 1999. Changes in muscle mass and phenotype and the expression of autocrine and systemic growth factors by muscle in response to stretch and overload. *J. Anat.* 194:323–334.

Granger, B.L., and E. Lazarides. 1979. Desmin and vimentin coexist at the periphery of the myofibril Z disc. *Cell*. 18:1053–1063.

Gredinger, E., A.N. Gerber, Y. Tamir, S.J. Tapscott, and E. Bengal. 1998. Mitogen-activated protein kinase pathway is involved in the differentiation of muscle cells. *J. Biol. Chem.* 273:10436–10444.

Grieff, M., M.P. Whyte, R.V. Thakker, and R. Mazzarella. 1997. Sequence analysis of 139 kb in Xp22.1 containing spermine synthase and the 5′ region of PEX. *Genomics*. 44:227–231.

Grow, M.W., and P.A. Krieg. 1998. Tinman function is essential for vertebrate heart development: elimination of cardiac differentiation by dominant inhibitory mutants of the *tinman*-related genes, *XNkx2-3* and *XNkx2-5*. *Dev. Biol.* 204:187–196.

Guo, L., J. Lynch, K. Nakamura, L. Fleigel, H. Kasahara, S. Izumo, I. Komuro, L.B. Agellon, and M. Michalak. 2000. COUP-TF1 antagonizes Nkx2.5-mediated activation of the calreticulin gene during cardiac development. *J. Biol. Chem.* 276:2797–2801.

Harvey, R.P. 1996. *NK-2* homeobox genes and heart development. *Dev. Biol.* 178:203–216.

Hirayama, E., M. Nakanishi, N. Honda, and J. Kim. 1999. Mouse C2 myoblasts resist HVJ (Sendai virus)-mediated cell fusion in the proliferating stage but become capable of fusion after differentiation. *Differentiation*. 64:213–223.

Kaibuchi, K., S. Kurodo, and M. Amano. 1999. Regulation of the cytoskeleton

and cell adhesion by the Rho family of GTPases in mammalian cells. *Annu. Rev. Biochem.* 68:459–486.

Lawlor, M.A., and P. Rotwein. 2000. Coordinate control of muscle cell survival by distinct insulin-like growth factor activated signalling pathways. *J. Cell Biol.* 151:1131–1140.

Layne, M.D., and S.R. Farmer. 1999. Tumor necrosis factor-α and basic fibroblast growth factor differentially inhibit the insulin-like growth factor-I induced expression of myogenin in C2C12 myoblasts. *Exp. Cell Res.* 249:177–187.

Luo, L., Y.J. Liao, L.Y. Jan, and Y.N. Jan. 1994. Distinct morphogenetic functions of similar small GTPases: *Drosophila* Drac1 is involved in axonal outgrowth and myoblast fusion. *Genes Dev.* 8:1787–1802.

Lyons, I., L.M. Parsons, L. Hartley, R. Li, J.E. Andrews, L. Robb, and R.P. Harvey. 1995. Myogenic and morphogenetic defects in the heart tubes of murine embryos lacking the homeobox gene *Nkx2-5*. *Genes Dev.* 9:1654–1666.

Millino, C., F. Sarinella, C. Tiveron, A. Villa, S. Sartore, and S. Ausoni. 2000. Cardiac and smooth muscle cell contributions to the formation of the murine pulmonary veins. *Dev. Dyn.* 218:414–425.

Molkentin, J.D., J.-R. Lu, C.L. Antos, B. Markham, J. Richardson, J. Robbins, S.R. Grant, and E.N. Olson. 1998. A calcineurin-dependent transcriptional pathway for cardiac hypertrophy. *Cell.* 93:215–228.

Musaro, A., and N. Rosenthal. 1999. Maturation of the myogenic program is induced by post-mitotic expression of IGF-1. *Mol. Cell. Biol.* 19:3115–3124.

Musaro, A., K.J.A. McCullagh, F.J. Naya, E.N. Olson, and N. Rosenthal. 1999. IGF-1 induces skeletal myocyte hypertrophy through calcineurin in association with GATA2 and NF-ATc1. *Nature.* 400:581–585.

Nobes, C.D., and A. Hall. 1995. Rho, Rac, and Cdc42 GTPases regulate the assembly of multimolecular focal complexes associated with actin stress fibers, lamellipodia, and filopodia. *Cell.* 81:53–62.

Pardo, J.V., J.D. Siliciano, and S.W. Craig. 1983. A vinculin-containing cortical lattice in skeletal muscle: transverse lattice elements ("costameres") mark sites of attachment between myofibrils and sarcolemma. *Proc. Natl. Acad. Sci. USA.* 80:1008–1012.

Park, M., C. Lewis, D. Turbay, A. Chung, J.N. Chen, S. Evans, R.E. Breitbart, M.C. Fishman, S. Izumo, and R. Bodmer. 1998. Differential rescue of visceral and cardiac defects in *Drosophila* by vertebrate tinman-related genes. *Proc. Natl. Acad. Sci. USA.* 95:9366–9371.

Patzak, D., O. Zhuchenko, C.-C. Lee, and M. Wehnert. 1999. Identification, mapping, and genomic structure of a novel X-chromosome human gene (SMPX) encoding a small muscular protein. *Hum. Genet.* 105:506–512.

Ranganayakulu, G., D.A. Elliot, R.P. Harvey, and E.N. Olson. 1998. Divergent roles for *NK-2* class homeobox genes in cardiogenesis in flies and mice. *Development.* 125:3037–3048.

Rivkees, S.A., M. Chen, J. Kulkarni, J. Browne, and Z. Zhao. 1999. Characterization of the murine A1 adenosine receptor promoter, potent regulation by GATA-4 and Nkx2.5. *J. Biol. Chem.* 274:14204–14209.

Rusnak, F., and P. Mertz. 2000. Calcineurin: form and function. *Physiol. Rev.* 80:1483–1521.

Schott, J.-J., D.W. Benson, C.T. Basson, W. Pease, G.M. Silberach, J.P. Moak, B.J. Maron, C.E. Seidman, and J.G. Seidman. 1998. Congenital heart disease caused by mutations in the transcription factor *NKX2-5*. *Science.* 281:108–111.

Schwenk, F., U. Baron, and K. Rajewsky. 1995. A Cre-transgenic mouse strain for the ubiquitous deletion of loxP-flanked gene segments including deletion in germ cells. *Nucleic Acids Res.* 23:5080–5081.

Semsarian, C., M.-J. Wu, Y.-K. Ju, T. Marciniec, T. Yeoh, D.G. Allen, R.P. Harvey, and R.M. Graham. 1999. Skeletal muscle hypertrophy is mediated by a Ca^{2+}-dependent calcineurin signalling pathway. *Nature.* 400:576–581.

Skerjanc, I.C., H. Peteropoulos, A.G. Ridgeway, and S. Wilton. 1998. Myocyte enhancer factor 2C and Nkx2-5 up-regulate each other's expression and initiate cardiomyogenesis in P19 cells. *J. Biol. Chem.* 273:34904–34910.

Sotiropoulos, A., D. Geneitis, J. Copeland, and R. Treisman. 1999. Signal-regulated activation of serum response factor is mediated by changes in actin dynamics. *Cell.* 98:159–169.

Tanaka, M., Z. Chen, S. Bartunkova, N. Yamasaki, and S. Izumo. 1999. The cardiac homeobox gene *Csx/Nkx2.5* lies genetically upstream of multiple genes for heart development. *Development.* 126:1269–1280.

Wu, H., F.J. Naya, T.A. McKinsey, B. Mercer, J.M. Shelton, E.R. Chin, A.R. Simard, R.N. Michel, R. Bassel-Duby, E.N. Olson, and R.S. Williams. 2000. MEF2 responds to multiple calcium-regulated signals in the control of skeletal muscle fiber type. *EMBO J.* 19:1963–1973.

Yagami-Hiromasa, T., T. Sato, T. Kurisaki, K. Kamijo, Y. Nabeshima, and A. Fujisawa-Sehara. 1995. A metalloprotease-disintegrin participating in myoblast fusion. *Nature.* 377:652–656.

Yotov, W.V., and R. St-Arnaud. 1996. Differential splicing-in of a proline-rich exon converts αNAC into a muscle-specific transcription factor. *Genes Dev.* 10:1763–1772.